separations

MDPI

Article

A Method for Purifying Pseudorabies Virus for Labeling the Neural Circuit by Using Capto™ Core 700

Rui Mei [1,2,†], Qinghan Wang [1,2,†], Kangyixin Sun [1,2], You Hu [1,2,3], Fuqiang Xu [1,2,3,4,5,6,*] and Fan Jia [1,2,3,7,*]

1 Guangdong Provincial Key Laboratory of Brain Connectome and Behavior, The Brain Cognition and Brain Disease Institute, Shenzhen-Hong Kong Institute of Brain Science-Shenzhen Fundamental Research Institutions, Shenzhen Institutes of Advanced Technology, Chinese Academy of Sciences, Shenzhen 518055, China; 2550243030@mails.szu.edu.cn (R.M.); qinghanwang1998@163.com (Q.W.); kangyixin1629@gmail.com (K.S.); y.hu@siat.ac.cn (Y.H.)
2 NMPA Key Laboratory for Research and Evaluation of Viral Vector Technology in Cell and Gene Therapy Medicinal Products, Key Laboratory of Quality Control Technology for Virus-Based Therapeutics, Guangdong Provincial Medical Products Administration, Shenzhen Key Laboratory of Viral Vectors for Biomedicine, Shenzhen Institutes of Advanced Technology, Chinese Academy of Sciences, Shenzhen 518055, China
3 University of Chinese Academy of Sciences, Beijing 100190, China
4 Innovation Academy for Precision Measurement Science and Technology, Chinese Academy of Sciences, Wuhan 430071, China
5 Center for Excellence in Brain Science and Intelligence Technology, Chinese Academy of Sciences, Shanghai 200031, China
6 Hubei Research Center of Fundamental Science-Chemistry, Wuhan 430074, China
7 Hubei Provincial Clinical Research Center for Alzheimer's Disease, Brain Science and Advanced Technology Institute, School of Medicine, Wuhan University of Science and Technology, Wuhan 430081, China
* Correspondence: fq.xu@siat.ac.cn (F.X.); fan.jia@wust.edu.cn (F.J.)
† These authors contributed equally to the work.

Abstract

Background: Viral vectors are indispensable tools in gene therapy and neural circuit mapping, offering promising therapeutic strategies for diverse genetic diseases and advancing neuroscience research. To achieve high transduction efficiency while mitigating impurity-induced immunogenicity, the development of viral vectors with improved purity and quality is essential. However, this critical requirement is often unmet by conventional purification methods such as ultracentrifugation, which are time-consuming and frequently result in limited product purity. The pseudorabies virus (PRV) is extensively employed as a viral tool for mapping neural circuits, where improved purity contributes to enhanced accuracy of neural tracing. PRV531 is a retrograde trans-synaptic tracer modified from the PRV Bartha strain, specifically designed to facilitate the precise visualization of hierarchical neural networks. Methods: In this study, we developed a method for the concentration and purification of PRV531 by integrating hollow fiber ultrafiltration (HF) with Capto™ Core 700 (CC700) chromatography. Initially, to concentrate the viral supernatant, a 500 kDa HF membrane was employed, maintaining a feed flow rate of 80 mL/min, a shear rate ranging from 2000 to 6000 s^{-1}, and a transmembrane pressure (TMP) between 0.5 and 1 bar. Following concentration, the virus underwent purification through CC700 chromatography, operating at linear flow rates ranging from 100 to 300 cm/h. Results: Sodium dodecyl sulfate–polyacrylamide gel electrophoresis (SDS-PAGE) revealed distinct bands consistent with the expected sizes of major PRV structural proteins, each with molecular weights ranging from 25 kDa to 150 kDa, concurrently demonstrating a substantial reduction in host cell proteins (HCPs) contamination. The purified PRV531 achieved a high final infectious titer of 3.55×10^9 PFU/mL, with an overall functional virus recovery of 8.88% from the crude supernatant to the final product. Conclusion: These data demonstrate that TFF combined with CC700 resin can efficiently purify retrograde trans-synaptic PRV tracer.

Check for updates

Academic Editors: Alberto Barbiroli and Evroula Hapeshi

Received: 28 April 2026
Revised: 4 June 2026
Accepted: 16 June 2026
Published: 19 June 2026

Copyright: © 2026 by the authors. Licensee MDPI, Basel, Switzerland. This article is an open access article distributed under the terms and conditions of the Creative Commons Attribution (CC BY) license.

Furthermore, this approach provides a promising strategy for purifying other viral-based tracers that traditionally rely on conventional centrifugation methods.

Keywords: pseudorabies virus; chromatographic technology; virus purification process; viral tracers

1. Introduction

Systematic breakthroughs in core technical aspects of viral vectors (encompassing engineering optimization, targeted delivery efficacy, and biosafety) have laid a pivotal foundation for the transformative advancement of gene therapy and neural circuit mapping. Consequently, engineered viral vectors have been extensively utilized in preclinical research and clinical interventions for a broad spectrum of systemic diseases and malignant tumors [1]. For mapping neural circuits, viral tracers like herpes simplex virus, pseudorabies virus (PRV), and rabies virus (RV) are extensively utilized [2–4]. Within this group, PRV functions as a highly efficient retrograde trans-synaptic tracer. PRV belongs to the family *Orthoherpesviridae*, subfamily *Alphaherpesvirinae*, and genus *Varicellovirus*, with its official species designation being *Suid herpesvirus 1* [5,6]. PRV comprises numerous strains, including the Becker and Bartha strains. PRV531 is a retrograde trans-synaptic tracer derived from the Bartha strain. Its high-level constitutive expression of enhanced green fluorescent protein (EGFP) substantially improves the detection and visualization of tracer signals [7]. PRV is an enveloped virus, whose envelope—consisting of a lipid bilayer and surface glycoproteins—displays high susceptibility to shear stress. This intrinsic property imposes stringent requirements on both operating parameters and process design during the purification workflow. Consequently, precise regulation of these critical factors is imperative to safeguard the structural integrity and infectivity of PRV particles [8].

Enhancing the purity of vectors, the effectiveness of transgenic expression, and the efficiency of transduction diminish the likelihood of detrimental immune reactions in the host post-vector injection. Adeno-associated virus vectors with higher purity demonstrate superior transduction efficiency [9]. Consequently, viral tracers with improved purity have been reported to facilitate more reliable neural labeling and may reduce nonspecific inflammatory responses. Present techniques for purifying viruses encompass gradient centrifugation with cesium chloride, sucrose, or iodixanol, ion-exchange chromatography, and multimodal chromatography, to name a few [10–12]. Capto^{TM} Core 700 (CC700) is a multimodal chromatography resin that integrates size-exclusion and binding mechanisms (ion-exchange and hydrophobic interactions). The resin consists of inert outer beads with a 700 kDa molecular weight cutoff. Viral particles larger than the pore size are excluded and recovered in the flow-through fraction, while smaller host cell proteins (HCPs) and nucleic acids enter the porous core and are captured by mixed-mode ligands [13]. The CC700 has a large particle size and complex surface composition, and is suitable for purifying enveloped viruses such as Japanese encephalitis virus, dengue virus, and RV [14–16]. The resin demonstrates a strong ability to bind to host cell proteins and DNA contaminants, simultaneously preserving elevated rates of virus recovery [17,18]. As a result, the process of CC700 purification offers virology labs a feasible way to acquire viral samples of greater purity compared to those obtained from raw cell lysates, culture mediums, or rapid pelleting [10].

In this study, we developed a technique to concentrate and purify PRV531. Given PRV531′s nature as an enveloped virus vulnerable to mechanical stress, preserving its structural soundness during processing is essential. Consequently, the choice of hollow fiber ultrafiltration (HF) in tangential flow filtration (TFF) mode for the concentration phase

aimed to reduce the impact of shear stress. Following concentration, the viral solution underwent purification with CC700, subsequent to which its purity and concentration were examined. To our knowledge, there are limited reports describing the purification of PRV531 using a hollow fiber system in conjunction with CC700 chromatography. As a result, this research lays the groundwork for fine-tuning essential purification factors to produce PRV531 with elevated titer and purity, vital for the creation of viral tracers in neural circuit studies.

2. Materials and Methods

2.1. Cells, Virus and Animals

The Baby Hamster Kidney-21 (BHK-21, CCL-10^{TM}) were purchased from the American Type Culture Collection (ATCC, Manassas, VA, USA). BHK-21 cells were cultured in Dulbecco's Modified Eagle Medium (DMEM, L110KJ, Basal Media, Shanghai, China), enriched with 10% fetal bovine serum (FBS, 10,091,148, Gibco, Auckland, New Zealand), and kept at 37 °C in an atmosphere containing 5% CO_2.

For virus propagation, BHK-21 cells were seeded into twenty 10 cm dishes at a density of 1×10^6 cells per dish and grown to 90% confluency prior to infection. The PRV531 strain used in this study is derived from the PRV Bartha vaccine strain and contains a triple-copy EGFP expression cassette inserted into the gG locus, as previously described [7]. Virus stocks were propagated in BHK-21 cells: the culture medium was replaced with DMEM containing 2% FBS, and PRV531 was inoculated at a multiplicity of infection of 0.1 into each 10 cm dish.

Male C57BL/6J mice (9–10 weeks old) were purchased from Vital River Co., Ltd. (Foshan, China). The C57BL mice resided in a controlled environment, experiencing a cycle of 12 h of light followed by 12 h of darkness, with unrestricted access to food and water for them. All studies were performed following the National Guidelines for the Care and Use of Laboratory Animals and approved by the Animal Care and Use Committees at the Shenzhen Institutes of Advanced Technology, Chinese Academy of Sciences (SIAT-IACUC-200303-NS-JF-A1071).

2.2. Virus Purification Process

At 48 h post-infection (hpi), the culture supernatant was harvested and clarified by 0.45 μm filtration. Subsequently, the viral supernatant concentrated and diafiltrated using a 500 kDa HF cartridge (D04-E500-05-N, Repligen, Waltham, MA, USA). This procedure utilized a buffer composed of 20 mM Tris and 150 mM NaCl, flowing at a rate of 80 mL/min. Control of the shear rate ranged from 2000 to 6000 s^{-1}, with the transmembrane pressure (TMP) consistently kept between 0.5 and 1 bar. Concentration of the supernatant ranged between 5 and 10 times.

Following concentration, the retentate was polished using an automated chromatography system equipped with a CC700 column (17548115, Cytiva, Marlborough, MA, USA) to deplete residual HCPs and host genomic DNA. Equilibration and elution buffers were composed of 20 mM Tris and 150 mM NaCl at a pH of 7.5, sustaining a flow rate ranging from 100 to 300 cm/h. The virus-containing flow-through fractions were pooled and subjected to HF ultrafiltration under identical buffer and flow conditions for preliminary volume reduction. Finally, the pooled sample was further concentrated to a final volume of 120 μL by centrifugation at 3000× *g* at 4 °C using 100 kDa centrifugal filter (Millipore, Billerica, MA, USA).

2.3. Plaque Assay and SDS-PAGE

The infectivity of all viral samples collected at different stages of the purification process, including the HF retentate, ÄKTA multimodal chromatography purification product (CC700 flowthrough pool), and the end product (purified PRV531), was determined by standard plaque assay on BHK-21 cells. BHK-21 cells were cultured in 6-well plates and subjected to a series of 10-fold dilutions of PRV supernatant for an hour at a temperature of 37 °C. Following this, each well received an initial layer of agar. At 48 hpi, an additional stratum of agar infused with neutral red (71,028,260, Sinopharm Chemical Reagent Co., Ltd., Shanghai, China) was introduced. Following an extra 24 h incubation period, the plaque count was measured. The viral concentrations were determined in terms of plaque-forming units per milliliter (PFU/mL).

The purified samples were evenly blended with a 5× concentration of loading buffer in a suitable proportion, subjected to denaturation at 95 °C for a duration of 10 min, and then separated using SDS-PAGE on a gel containing 4–20% polyacrylamide. Following this, the gels were colored using a solution of 5% Coomassie Brilliant Blue, which included 25% methanol and 5% glacial acetic acid.

2.4. Stereotaxic Microinjection into the Brains of Mice

The purified PRV531 was adjusted to a working titer of 1×10^9 PFU/mL using sterile phosphate-buffered saline (PBS). Eight-week-old male mice (n = 3) received a stereotaxic microinjection of PRV531 (300 nL) targeted into the ventral hippocampus (VHPC). At 60 hpi, the mice were deeply anesthetized via an intraperitoneal injection of sodium pentobarbital (100 mg/kg) and transcardially perfused with PBS, followed by 4% paraformaldehyde (PFA) in PBS. Extracted brain tissues were post-fixed overnight in 4% PFA at 4 °C, cryoprotected in 30% sucrose-PBS, and cut into 40 μm coronal sections using a cryostat microtome (CM1950, Leica, Wetzlar, Germany). Tissue sections were imaged and analyzed using a confocal laser scanning microscope (LSM 900, ZEISS, Oberkochen, Germany).

3. Results

3.1. Overview of the PRV531 Purification Workflow

At 48 hpi, the virus-containing culture medium was harvested and clarified using a 0.45 μm filter. The supernatant was subsequently concentrated and subjected to buffer exchange utilizing HF ultrafiltration. The core purification step applied CC700 multimodal chromatography to efficiently deplete HCPs and host DNA contaminants in flow-through mode. Finally, the polished virus fraction underwent a HF concentration and was further formulated to a micro-volume via centrifugal ultrafiltration. The detailed schematic of this sequential downstream process is illustrated in Figure 1.

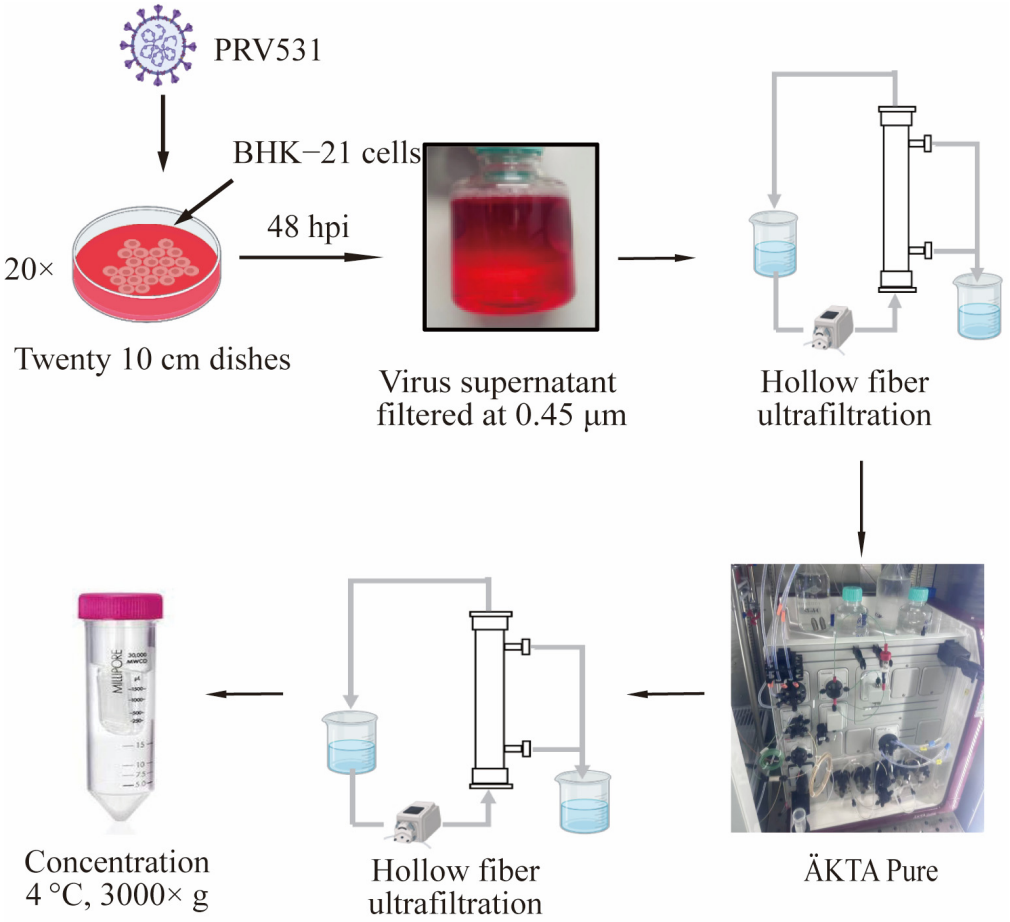


Figure 1. Diagram of the PRV purification strategy based on CC700 chromatography. The BHK-21 cells were infected with PRV531 in twenty 10 cm dishes for 48 h. The virus-containing supernatant is then filtered through a 0.45 μm filter, concentrated by HF, and further purified using CC700 chromatography. Virus-containing flow-through fractions were concentrated via HF ultrafiltration under identical conditions. Finally, the purified virus is collected and concentrated by centrifugation (3000× *g* at 4 °C) to obtain the final product. Arrows indicate the sequential processing steps of virus preparation.

3.2. Chromatographic Elution Profile of PRV531

As depicted in Figure 1, the virus underwent purification. Displayed in Figure 2 are the ultraviolet absorption patterns at 280 nm and 260 nm, along with the conductivity and the 260/280 ratio of PRV531 during the purification process. Within the flow-through volume range of 15–75 mL, the 260/280 ratio remained stable at a value between 1.0 and 1.2 (Figure 2D), indicating that the ratio of protein to nucleic acid in each collection tube was stable and consistent with the elution characteristics of the virus particles. A small flow-through peak of approximately 250 milli-absorption units (mAU) was observed at the wavelengths of 280 nm and 260 nm (marked as 'collected' in Figure 2A,B) [10], further suggesting that this peak corresponds to the peak position of the virus particles. As a result, the segments that eluted from 15 mL to 75 mL were combined for further concentration and purification.

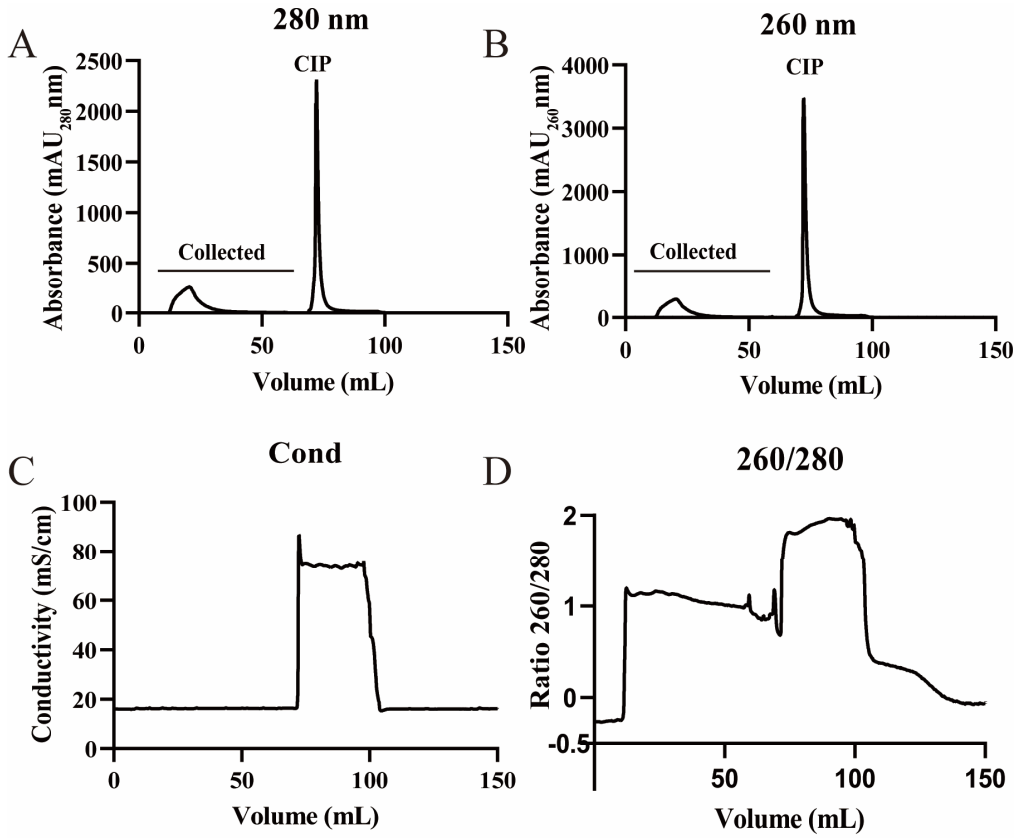


Figure 2. Viral chromatographic elution profiles: (**A**) chromatogram showing milli-absorption units (mAU) at 280 nm for each 1 mL fraction during collection and cleaning-in-place (CIP); (**B**) chromatogram showing mAU at 260 nm for each 1 mL fraction during collection and CIP; (**C**) electrical conductivity; (**D**) 260/280 absorbance ratio.

3.3. Titer and Purity of PRV531

During PRV's purification, the titers of the HF Retentate, CC700 flowthrough pool, and the purified PRV531 were evaluated using plaque assay and SDS-PAGE. Findings showed that HF Retentate, CC700 flowthrough pool, and purified PRV531 all resulted in plaque morphology remained consistent in size and distribution (Figure 3A). The CC700 purified sample, when stained with Coomassie blue, revealed multiple prominent protein bands with molecular weights around 150 kDa, 100 kDa, 80–70 kDa, 70–60 kDa, and 35–25 kDa. These bands are consistent with expected sizes of major PRV structural proteins (Figure 3B) [19]. The findings revealed that the PRV531 virus, purified through HF and CC700 chromatography, showed high infectivity and reduced protein contamination.

Total infectivity (total PFU) and stepwise recovery rates were then determined based on these averaged titers. The unpurified PRV531 virus (200 mL, 1.0×10^8 PFU/mL) contained 2.0×10^{10} PFU. After HF, the HF retentate (10 mL, 4.65×10^8 PFU/mL) yielded a total PFU of 4.65×10^9, corresponding to a stepwise recovery of 23.25% relative to the starting material. The subsequent CC700 flow-through pool (50 mL, 1.0×10^8 PFU/mL) contained 5.00×10^9 PFU, representing a stepwise recovery of 107.53% relative to the previous step. The final purified product was concentrated into 0.5 mL, achieving a high-titer concentrate of 3.55×10^9 PFU/mL with a total PFU of 1.78×10^9, and a stepwise recovery of 35.50% relative to the CC700 flow-through pool. The overall recovery from the unpurified PRV531 virus to the final purified product was 8.88%, demonstrating the efficiency of the developed workflow (Table 1).

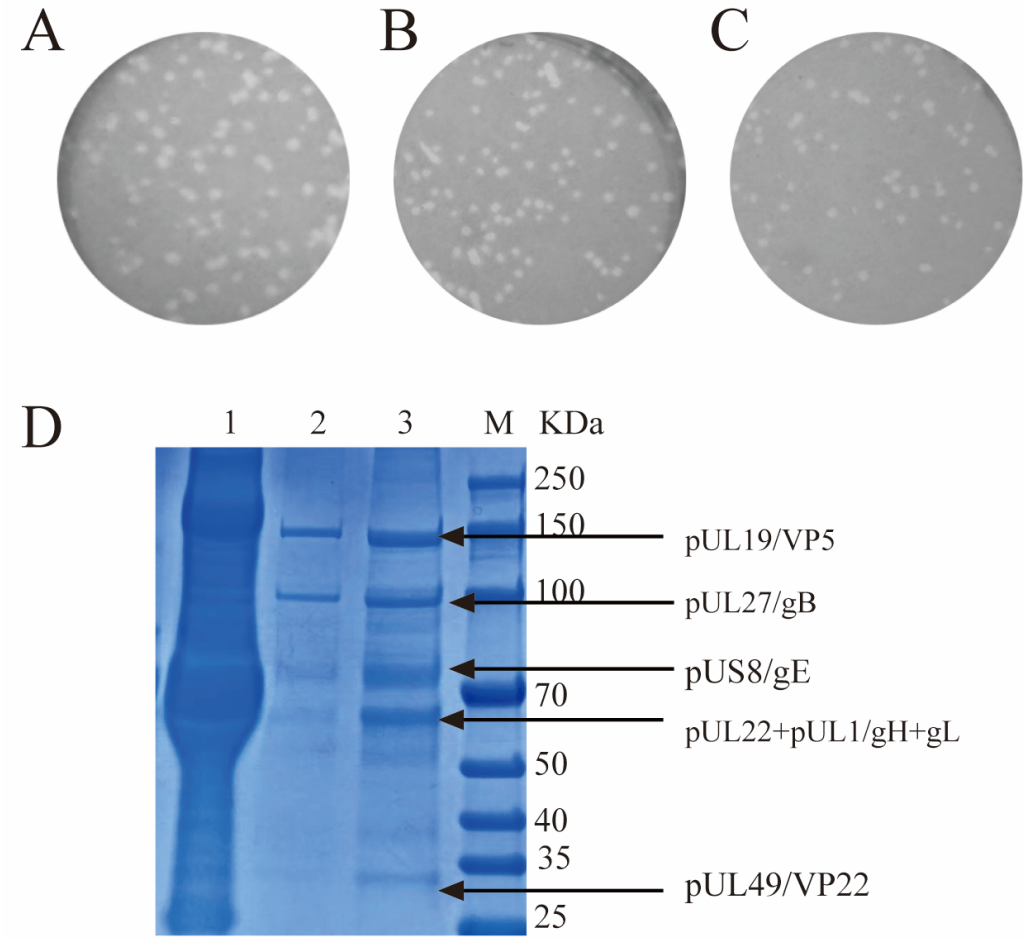


Figure 3. Titration and purity assessment of the virus samples. (**A**–**C**) Plaque assay of PRV531 samples at different stages. The panels show the HF Retentate (**A**), CC700 flow-through pool (**B**), and the final purified PRV531 (**C**). (**D**) Purity evaluation of viral particles by SDS-PAGE. M: Protein Marker; Lane 1, HF Retentate; Lane 2, CC700 flow-through pool; Lane 3, Purified PRV531.

Table 1. Total viral PFU and step-wise recovery rates during hollow fiber ultrafiltration and chromatography purification.

Sample Name	Volume (mL)	Average Titer (PFU/mL)	Total PFU	Relative to the Previous Step's Recovery Rate	Relative to the Initial Total Recovery Rate
Unpurified PRV531 virus	200	1.00×10^8	2.0×10^{10}		
HF Retentate	10	4.65×10^8	4.65×10^9	23.25%	23.25%
CC700 flowthrough pool	50	1.00×10^8	5.00×10^9	107.53%	25.00%
Purified PRV531	0.5	3.55×10^9	1.78×10^9	35.50%	8.88%

3.4. PRV531 Mediates Robust Retrograde Tracing In Vivo

PRV531 was injected into the VHPC of the mouse brain. Enhanced green fluorescent protein (EGFP)-positive neurons were observed in the VHPC. Key labeled areas included the reuniens thalamic nucleus (Re), piriform cortex (Pir), nucleus of the diagonal band (NDB), medial septal nucleus (MS), lateral septal nucleus intermediate part (LSl), lateral preoptic area (LPO), lateral hypothalamic area (LH), laterodorsal thalamic nucleus (LD), and the anterior part of the basolateral amygdaloid nucleus (BLA) (Figure 4).

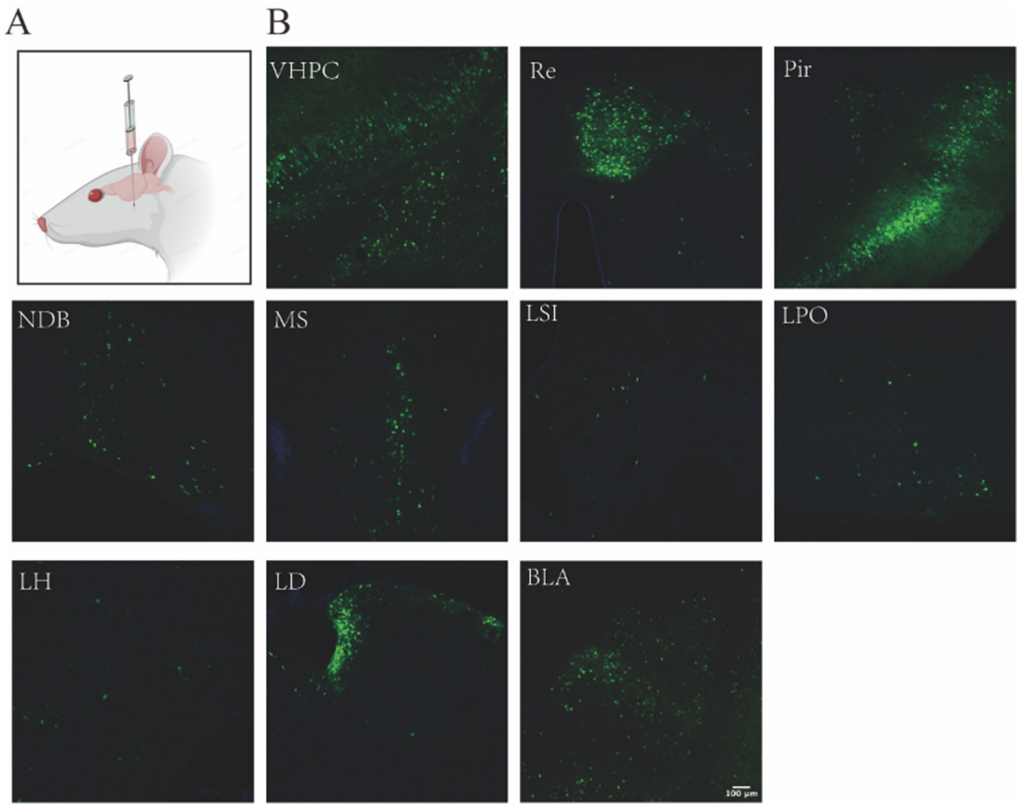


Figure 4. Retrograde Tracing of PRV 531 in the Mouse VHPC. (**A**) Schematic illustration of PRV 531 injection. (**B**) PRV 531 (1×10^9 PFU/mL, 300 nL) was delivered into the VHPC of mice. At 60 hpi, brains were processe and sectioned, and EGFP expression was observed in various brain regions.

Crucially, this retrograde labeling pattern matched the well-documented topological anatomy of hippocampal afferent circuits [20,21]. The trans-synaptic signal distribution mapping the septal, thalamic, and limbic connections accurately reflected previously verified mono- and multi-synaptic projection pathways [22,23]. These neuroanatomical mapping results verify that the CC700-purified PRV531 retains reliable retrograde tracing fidelity.

4. Discussion

This study established an efficient purification approach for PRV531 using CC700 chromatography. This technique integrates size exclusion and adsorption principles, enabling the removal of small molecular contaminants while allowing large viral particles to pass through the column. The distinctive design of CC700, comprising an inactive outer shell and an inner core functionalized with ligands, facilitates the capture of host cell proteins and nucleic acid impurities within the core, while viral particles (>700 kDa) are recovered in the flow-through fraction [24]. This dual mechanism makes the purification process rapid, scalable, and compatible with diverse viral systems. Previous studies have demonstrated that CC700 effectively reduces host-derived impurities in vaccine and extracellular vesicle purification. For instance, in flavivirus vaccine production, combining anion-exchange membrane adsorption (Sartobind Q) with CC700 chromatography reduced residual DNA to 1.3 ± 1.6 ng/dose and host cell proteins to 345 ± 25 ppm, achieving a virus recovery rate of approximately 53% [25]. Likewise, in exosome isolation, CC700 preserved vesicle integrity and particle size better than ultracentrifugation, maintaining nearly 80% recovery and comparable purity and biological activity [26]. These reports support the use of CC700 as a versatile platform for purifying complex biological nanoparticles.

Traditional purification of enveloped viruses such as PRV mainly relies on sucrose cushion ultracentrifugation, which achieves separation based on density sedimentation [27]. However, this method is laborious, time-consuming, non-scalable, and prone to causing viral aggregation and loss of infectivity due to high hydrostatic pressure and hyperosmotic stress [28–30]. In this study, we established a coupled purification process consisting of TFF and CC700 chromatography. TFF provides a low-shear environment for concentration and clarification while protecting the viral envelope [31]. CC700 uses a flow-through mode to purify viruses based on size exclusion, efficiently removing residual host proteins and nucleic acids without damaging viral structure [10,32]. This combined strategy significantly reduces the load and cost of chromatographic media [33,34]. A comparative summary is provided in Table 2.

Table 2. Comparison of traditional ultracentrifugation and the TFF and CC700 coupled process for virus purification.

Parameter	Sucrose Cushion Ultracentrifugation	TFF and CC700 Chromatography
Separation principle	Density-dependent sedimentation [27]	Size exclusion and core ligand capture [10,32]
Viral shear stress	High, risk of aggregation [28–30]	Low, protects envelope integrity [31]
Recovery	Unstable, titer loss common [35]	High, well-preserved [35]
Impurity removal	Moderate, co-sedimentation prone [36]	High, efficient HCP/DNA clearance [10]
Operation mode	Manual, time-consuming [37]	Automated, time-saving [37]
Scalability	Poor, lab-scale only [28]	Excellent, industrial-compatible [33,34]

In our methodology, the average virion diameter of PRV531 (150–180 nm) exquisitely matched the molecular exclusion threshold of CC700. The procedure was enacted at a conservative linear flow rate of 100–300 cm/h following HF ultrafiltration at a constrained shear rate of 2000–6000 s^{-1}. While a nominal titer attrition was incurred, downstream qualitative SDS-PAGE analysis indicated a profound clearance of host-contaminating proteins (Figure 3B). The lower flow rate favored impurity clearance by extending the contact time between contaminants and the resin ligands, consistent with previous findings [24]. Compared with other core-based chromatographic media, such as Capto Core 400, which is better suited for smaller viral particles (<80 nm), CC700 appeared more suitable for PRV531 purification due to its larger pore size distribution. Furthermore, while TFF offers advantages in concentration and buffer exchange for shear-sensitive biomolecules [38,39], CC700 provides a more effective polishing step to achieve preparations with improved purity suitable for downstream applications.

Despite the demonstrated efficacy of the purification of PRV531, the final purified product recovery rate of PRV531 was approximately 8.88% (Figure 3C). To address this limitation and further optimize the purification process, future efforts should consider the biophysical fragility of large enveloped viruses. Rearranging the purification sequence by performing CC700 chromatography prior to TFF may alleviate membrane fouling. Studies on similar enveloped viruses, such as respiratory syncytial virus (RSV), have shown that removing over 99% of HCPs via negative-mode chromatography before concentration substantially reduces viscosity-induced resistance during TFF [40]. This tactical inversion could be further reinforced by executing an early-stage Benzonase digestion step (catalyzed by 5 mM $MgCl_2$) to chop host genomic DNA networks, subsequently silencing localized electrostatic aggregation [41]. Additionally, the physical stress imposed on the viral envelope during TFF requires rigorous parameter control. To prevent the entrapment of PRV particles (approximately 150–200 nm in diameter), transmembrane pressure (TMP) should be maintained below 4 psi (approximately 0.027 MPa), with a shear rate controlled between 2000 and 4000 s^{-1} to balance membrane flux and preserve envelope integrity [42].

Upgrading the membrane molecular weight cut-off from 500 kDa to 750 kDa may also improve permeate flux. From a biochemical stability perspective, all operations should be performed at 4 °C and completed within a compressed 4 h timeframe to counteract the rapid titer decay typical of herpesviruses. The inclusion of stabilizing excipients, such as 10% sorbitol or ultra-low concentrations of non-ionic surfactants (e.g., 0.005–0.01% Tween-80), could minimize non-specific viral adsorption to equipment surfaces without compromising the lipid envelope [43]. Collectively, integrating these sequence adjustments, parameter constraints, and formulation enhancements is expected to synergistically improve PRV recovery and infectivity in future applications.

5. Conclusions

In summary, the purification of PRV531 using the TFF coupled with CC700 resin achieved a balance between recovery and purity. This work establishes a methodological basis for optimizing operational parameters and future scale-up of PRV production for subsequent biological and structural studies. Nevertheless, this study is limited by the lack of quantitative assessment of residual host cell DNA and proteins, which warrants further investigation.

Author Contributions: Conceptualization, F.J. and F.X.; methodology, K.S. and F.J.; formal analysis, R.M.; investigation, Y.H.; resources, F.J. and F.X.; data curation, R.M., Y.H. and Q.W.; writing—original draft preparation, R.M.; writing—review and editing, F.J., R.M. and K.S.; supervision, F.J.; project administration, F.J., R.M. and Q.W.; funding acquisition, F.J. and F.X. All authors have read and agreed to the published version of the manuscript.

Funding: This work was supported by the Brain Science and Brain-like Intelligence Technology-National Science and Technology Major Project: 2021ZD0201003; National Natural Science Foundation of China: 82441052; National Natural Science Foundation of China: 32071038; Shenzhen Fundamental Research Program: JCYJ20250604183134044; Shenzhen Fundamental Research Program: JCYJ20220818100801002; the Shenzhen Key Laboratory of Viral Vectors for Biomedicine: ZDSYS20200811142401005; and the SIAT Innovation Program for Excellent Young Researchers: E1G023.

Data Availability Statement: Data will be made available upon request.

Conflicts of Interest: The authors declare no conflicts of interest.

References

1. Bulcha, J.T.; Wang, Y.; Ma, H.; Tai, P.W.L.; Gao, G. Viral vector platforms within the gene therapy landscape. *Signal Transduct. Target. Ther.* **2021**, *6*, 53. [CrossRef] [PubMed]
2. Zhang, G.R.; Zhao, H.; Muneer, P.M.A.; Cao, H.; Li, X.; Geller, A.I. Neurons can be labeled with unique hues by helper virus-free HSV-1 vectors expressing Brainbow. *J. Neurosci. Methods* **2015**, *240*, 77–88. [CrossRef] [PubMed]
3. Li, B.; Zhu, L.; Zhou, Y.C.; Guo, W.Z.; Xu, Z.W. Studies on neuronal tracing with pseudorabies virus. *Chin. J. Virol.* **2014**, *30*, 333–337. [CrossRef]
4. Kelly, R.M.; Strick, P.L. Rabies as a transneuronal tracer of circuits in the central nervous system. *J. Neurosci. Methods* **2000**, *103*, 63–71. [CrossRef] [PubMed]
5. Davison, A.J.; Eberle, R.; Ehlers, B.; Hayward, G.S.; McGeoch, D.J.; Minson, A.C.; Pellett, P.E.; Roizman, B.; Studdert, M.J.; Thiry, E. The order Herpesvirales. *Arch. Virol.* **2009**, *154*, 171–177. [CrossRef] [PubMed]
6. Mettenleiter, T.C. Molecular biology of pseudorabies (Aujeszky's disease) virus. *Comp. Immunol. Microbiol. Infect. Dis.* **1991**, *14*, 151–163. [CrossRef] [PubMed]
7. Jia, F.; Lv, P.; Miao, H.; Shi, X.; Mei, H.; Li, L.; Xu, X.; Tao, S.; Xu, F. Optimization of the Fluorescent Protein Expression Level Based on Pseudorabies Virus Bartha Strain for Neural Circuit Tracing. *Front. Neuroanat.* **2019**, *13*, 63. [CrossRef] [PubMed]
8. Schimek, A.; Ng, J.K.M.; Hubbuch, J. Navigating the Purification Process: Maintaining the Integrity of Replication-Competent Enveloped Viruses. *Vaccines* **2025**, *13*, 444. [CrossRef] [PubMed]

9. Ayuso, E.; Mingozzi, F.; Montane, J.; Leon, X.; Anguela, X.M.; Haurigot, V.; Edmonson, S.A.; Africa, L.; Zhou, S.; High, K.A.; et al. High AAV vector purity results in serotype- and tissue-independent enhancement of transduction efficiency. *Gene Ther.* **2010**, *17*, 503–510. [CrossRef] [PubMed]
10. James, K.T.; Cooney, B.; Agopsowicz, K.; Trevors, M.A.; Mohamed, A.; Stoltz, D.; Hitt, M.; Shmulevitz, M. Novel High-throughput Approach for Purification of Infectious Virions. *Sci. Rep.* **2016**, *6*, 36826. [CrossRef] [PubMed]
11. Allmaier, G.; Blaas, D.; Bliem, C.; Dechat, T.; Fedosyuk, S.; Gösler, I.; Kowalski, H.; Weiss, V.U. Monolithic anion-exchange chromatography yields rhinovirus of high purity. *J. Virol. Methods* **2018**, *251*, 15–21. [CrossRef] [PubMed]
12. Halan, V.; Maity, S.; Bhambure, R.; Rathore, A.S. Multimodal Chromatography for Purification of Biotherapeutics—A Review. *Curr. Protein Pept. Sci.* **2019**, *20*, 4–13. [CrossRef] [PubMed]
13. Winter, D.L.; Lebhar, H.; McCluskey, J.B.; Glover, D.J. A versatile multimodal chromatography strategy to rapidly purify protein nanostructures assembled in cell lysates. *J. Nanobiotechnol.* **2023**, *21*, 66. [CrossRef] [PubMed]
14. Zhang, F.; Luo, J.; Teng, M.; Xing, G.; Guo, J.; Zhang, Y. Purification of cell-derived Japanese encephalitis virus by dual-mode chromatography. *Biotechnol. Appl. Biochem.* **2021**, *68*, 547–553. [CrossRef]
15. Sundaram, A.K.; Ewing, D.; Blevins, M.; Liang, Z.; Sink, S.; Lassan, J.; Raviprakash, K.; Defang, G.; Williams, M.; Porter, K.R.; et al. Comparison of purified psoralen-inactivated and formalin-inactivated dengue vaccines in mice and nonhuman primates. *Vaccine* **2020**, *38*, 3313–3320. [CrossRef] [PubMed]
16. Trabelsi, K.; Ben Zakour, M.; Kallel, H. Purification of rabies virus produced in Vero cells grown in serum free medium. *Vaccine* **2019**, *37*, 7052–7060. [CrossRef] [PubMed]
17. Lothert, K.; Pagallies, F.; Feger, T.; Amann, R.; Wolff, M.W. Selection of chromatographic methods for the purification of cell culture-derived Orf virus for its application as a vaccine or viral vector. *J. Biotechnol.* **2020**, *323*, 62–72. [CrossRef] [PubMed]
18. Lothert, K.; Pagallies, F.; Eilts, F.; Sivanesapillai, A.; Hardt, M.; Moebus, A.; Feger, T.; Amann, R.; Wolff, M.W. A scalable downstream process for the purification of the cell culture-derived Orf virus for human or veterinary applications. *J. Biotechnol.* **2020**, *323*, 221–230. [CrossRef] [PubMed]
19. Kramer, T.; Greco, T.M.; Enquist, L.W.; Cristea, I.M. Proteomic characterization of pseudorabies virus extracellular virions. *J. Virol.* **2011**, *85*, 6427–6441. [CrossRef] [PubMed]
20. Tao, S.; Wang, Y.; Peng, J.; Zhao, Y.; He, X.; Yu, X.; Liu, Q.; Jin, S.; Xu, F. Whole-Brain Mapping the Direct Inputs of Dorsal and Ventral CA1 Projection Neurons. *Front. Neural Circuits* **2021**, *15*, 643230. [CrossRef] [PubMed]
21. Prasad, J.A.; Chudasama, Y. Viral tracing identifies parallel disynaptic pathways to the hippocampus. *J. Neurosci.* **2013**, *33*, 8494–8503. [CrossRef] [PubMed]
22. Ohara, S.; Sato, S.; Tsutsui, K.; Witter, M.P.; Iijima, T. Organization of multisynaptic inputs to the dorsal and ventral dentate gyrus: Retrograde trans-synaptic tracing with rabies virus vector in the rat. *PLoS ONE* **2013**, *8*, e78928. [CrossRef]
23. Castle, M.; Comoli, E.; Loewy, A.D. Autonomic brainstem nuclei are linked to the hippocampus. *Neuroscience* **2005**, *134*, 657–669. [CrossRef] [PubMed]
24. Wood, L.D.; Parsons, D.W.; Jones, S.; Lin, J.; Sjöblom, T.; Leary, R.J.; Shen, D.; Boca, S.M.; Barber, T.; Ptak, J.; et al. The genomic landscapes of human breast and colorectal cancers. *Science* **2007**, *318*, 1108–1113. [CrossRef] [PubMed]
25. Pato, T.P.; Souza, M.C.O.; Mattos, D.A.; Caride, E.; Ferreira, D.F.; Gaspar, L.P.; Freire, M.S.; Castilho, L.R. Purification of yellow fever virus produced in Vero cells for inactivated vaccine manufacture. *Vaccine* **2019**, *37*, 3214–3220. [CrossRef] [PubMed]
26. Li, P.; Kaslan, M.; Lee, S.H.; Yao, J.; Gao, Z. Progress in Exosome Isolation Techniques. *Theranostics* **2017**, *7*, 789–804. [CrossRef] [PubMed]
27. Wong, M.-L.; Chen, C.-H. Evidence for the internal location of actin in the pseudorabies virion. *Virus Res.* **1998**, *56*, 191–197. [CrossRef] [PubMed]
28. Nestola, P.; Peixoto, C.; Silva, R.R.J.S.; Alves, P.M.; Mota, J.P.B.; Carrondo, M.J.T. Improved virus purification processes for vaccines and gene therapy. *Biotechnol. Bioeng.* **2015**, *112*, 843–857. [CrossRef] [PubMed]
29. Peixoto, C.; Sousa, M.F.Q.; Silva, A.C.; Carrondo, M.J.T.; Alves, P.M. Downstream processing of triple layered rotavirus like particles. *J. Biotechnol.* **2007**, *127*, 452–461. [CrossRef] [PubMed]
30. Segura, M.M.; Kamen, A.A.; Garnier, A. Overview of Current Scalable Methods for Purification of Viral Vectors. In *Viral Vectors for Gene Therapy: Methods and Protocols*; Merten, O.-W., Al-Rubeai, M., Eds.; Humana Press: Totowa, NJ, USA, 2011; pp. 89–116.
31. Grzenia, D.L.; Carlson, J.O.; Wickramasinghe, S.R. Tangential flow filtration for virus purification. *J. Membr. Sci.* **2008**, *321*, 373–380. [CrossRef]
32. Jungbauer, A.; Hahn, R. Monoliths for fast bioseparation and bioconversion and their applications in biotechnology. *J. Sep. Sci.* **2004**, *27*, 767–778. [CrossRef] [PubMed]
33. Konz, J.O.; Pitts, L.R.; Sagar, S.L. Scaleable Purification of Adenovirus Vectors. In *Gene Therapy Protocols: Design and Characterization of Gene Transfer Vectors*; Le Doux, J.M., Ed.; Humana Press: Totowa, NJ, USA, 2008; pp. 13–23.
34. Kramberger, P.; Urbas, L.; Štrancar, A. Downstream processing and chromatography based analytical methods for production of vaccines, gene therapy vectors, and bacteriophages. *Hum. Vaccines Immunother.* **2015**, *11*, 1010–1021. [CrossRef] [PubMed]

35. de las Mercedes Segura, M.; Kamen, A.; Garnier, A. Downstream processing of oncoretroviral and lentiviral gene therapy vectors. *Biotechnol. Adv.* **2006**, *24*, 321–337. [CrossRef] [PubMed]
36. Morenweiser, R. Downstream processing of viral vectors and vaccines. *Gene Ther.* **2005**, *12*, S103–S110. [CrossRef] [PubMed]
37. Wolf, M.W.; Reichl, U. Downstream processing of cell culture-derived virus particles. *Expert Rev. Vaccines* **2011**, *10*, 1451–1475. [CrossRef] [PubMed]
38. Negrete, A.; Pai, A.; Shiloach, J. Use of hollow fiber tangential flow filtration for the recovery and concentration of HIV virus-like particles produced in insect cells. *J. Virol. Methods* **2014**, *195*, 240–246. [CrossRef] [PubMed]
39. Hao, X.; Horax, R.; Qian, X.; Wheeler, A.; Shirataki, H.; Wickramasinghe, S.R. Harvesting AAV by tangential flow filtration using reverse asymmetric membranes. *Biotechnol. Prog.* **2025**, *41*, e70059. [CrossRef] [PubMed]
40. Mundle, S.T.; Kishko, M.; Groppo, R.; DiNapoli, J.; Hamberger, J.; McNeil, B.; Kleanthous, H.; Parrington, M.; Zhang, L.; Anderson, S.F. Core bead chromatography for preparation of highly pure, infectious respiratory syncytial virus in the negative purification mode. *Vaccine* **2016**, *34*, 3690–3696. [CrossRef] [PubMed]
41. Lagoutte, P.; Mignon, C.; Donnat, S.; Stadthagen, G.; Mast, J.; Sodoyer, R.; Lugari, A.; Werle, B. Scalable chromatography-based purification of virus-like particle carrier for epitope based influenza A vaccine produced in *Escherichia coli*. *J. Virol. Methods* **2016**, *232*, 8–11. [CrossRef] [PubMed]
42. Wickramasinghe, S.R.; Kalbfuß, B.; Zimmermann, A.; Thom, V.; Reichl, U. Tangential flow microfiltration and ultrafiltration for human influenza A virus concentration and purification. *Biotechnol. Bioeng.* **2005**, *92*, 199–208. [CrossRef] [PubMed]
43. Dayaram, A.; Franz, M.; Schattschneider, A.; Damiani, A.M.; Bischofberger, S.; Osterrieder, N.; Greenwood, A.D. Long term stability and infectivity of herpesviruses in water. *Sci. Rep.* **2017**, *7*, 46559. [CrossRef] [PubMed]

Disclaimer/Publisher's Note: The statements, opinions and data contained in all publications are solely those of the individual author(s) and contributor(s) and not of MDPI and/or the editor(s). MDPI and/or the editor(s) disclaim responsibility for any injury to people or property resulting from any ideas, methods, instructions or products referred to in the content.